# Impairment of substrate-mediated mitochondrial respiration in cardiac cells by chloroquine

Sivasailam Ashok[1] · Sasikala Rajendran Raji[1] · Shankarappa Manjunatha[2] · Gopala Srinivas[1]

## Abstract

Chloroquine (CQ) has a long clinical history as an anti-malarial agent and also being used for the treatment of other infections and autoimmune diseases. Recently, this lysosomotropic agent and its derivatives are also been tested as adjuncts alongside conventional anti-cancer treatments in combinatorial therapies. However, their reported cardiotoxicity tends to raise concern over their indiscriminate use. Even though the influence of CQ and its derivatives on cardiac mitochondria is extensively studied in disease models, their impact on cardiac mitochondrial respiration under physiological conditions remains inconclusive. In this study, we aimed to evaluate the impact of CQ on cardiac mitochondrial respiration using both in-vitro and in-vivo model systems. Using high-resolution respirometry in isolated cardiac mitochondria from male C57BL/6 mice treated with intraperitoneal injection of 10 mg/kg/day of CQ for 14 days, CQ was found to impair substrate-mediated mitochondrial respiration in cardiac tissue. In an in-vitro model of H9C2 cardiomyoblasts, incubation with 50 μM of CQ for 24 h disrupted mitochondrial membrane potential, produced mitochondrial fragmentation, decreased mitochondrial respiration and induced superoxide generation. Altogether, our study results indicate that CQ has a deleterious impact on cardiac mitochondrial bioenergetics which in turn suggests that CQ treatment could be an added burden, especially in patients affected with diseases with underlying cardiac complications. As CQ is an inhibitor of the lysosomal pathway, the observed effect could be an outcome of the accumulation of dysfunctional mitochondria due to autophagy inhibition.

**Keywords** Chloroquine · Heart · High-resolution respirometry · Mitochondria · Metabolism

## Introduction

CQ and its derivatives are the only FDA-approved drugs that have a direct inhibitory effect on autophagic flux [1–3]. Due to their weak basic nature, they are believed to get trapped into acidic cellular compartments such as endo-lysosomes, Golgi apparatus, etc., which provides a strong rationale for their use against various intracellular pathogens [4]. These properties also make them a potential choice for drug repurposing against various viral pathogens and as combinatorial therapies alongside anticancer agents [5–7].

Numerous reports have shown cardiac complications attributed to the use of CQ and its derivatives [8], even with minor daily dosage contributing towards mild to severe conduction disorders and cardio-vascular complications including vasodilation, hypotension, myocardial dysfunction, and arrhythmias [8–10]. Acute high-dose CQ as well as chronic low-dose CQ treatment for various disease conditions has been shown to cause a significant decline in myocardial efficiency with decreased aortic output [9, 11].

Terminally differentiated myocardial cells preserve their homeostasis through the intricate harmonization of various quality control pathways, the most important one being autophagy [12–14]. Any derangement in these pathways would affect mitochondrial homeostasis and can thus result in metabolic derangement. Impairment of the autophagic process has been linked to cardiac dysfunction associated with CQ [15]. In the subcellular context, CQ and its derivatives are shown to induce structural as well as functional

✉ Shankarappa Manjunatha
drmanjunatha@gmail.com

✉ Gopala Srinivas
srinivasg@sctimst.ac.in

1 Department of Biochemistry, Sree Chitra Tirunal Institute for Medical Sciences and Technology, Thiruvananthapuram, Kerala 695011, India

2 Dr B C Roy Multispeciality Medical Research Centre, Indian Institute of Technology, Kharagpur, Kharagpur 721302, India

abnormalities in mitochondria [16–20] in various model systems. Since heart tissue is heavily reliant on mitochondrial metabolism, any derangements to mitochondrial homeostasis could affect mitochondrial function and would ultimately result in cardiac complications [21]. However, the impact of CQ on mitochondrial respiration in healthy heart tissue remains unexplored. Therefore, this study largely aimed to assess the impact of CQ on mitochondrial function in a physiologically normal heart by targeting key parameters of mitochondrial respiratory functions using both in-vivo and in-vitro model systems. We found that CQ treatment altered the mitochondrial quality resulting in a decline in respiratory functions in cardiac cells.

## Materials and methods

### Animal experiment

Male C57BL/6 mice aged 8 weeks and body weight 30–40 g were included in the study and maintained in a specific pathogen-free facility with recommended temperature and humidity, on a 12:12 h light–dark cycle, with free access to standard diet and water. 10 mg/kg/day of CQ, equivalent to a human dose of 0.81 mg/kg/day [11] was injected intraperitoneally for 14 days, while the control group received saline. On completion of the intervention period, animals were euthanized and whole heart was extracted in ice-cold biopsy preservation solution (BIOPS) buffer followed by mitochondrial isolation [22]. Freshly isolated mitochondria were used for respiration measurements. Animal experiments were conducted with the approval of the Committee for the Purpose of Control and Supervision of Experiments on Animals (CPCSEA), Government of India, and the Institutional Animal Ethics Committee of Sree Chitra Tirunal Institute for Medical Sciences and Technology (SCTIMST), Trivandrum.

### High-resolution respirometry with isolated mitochondria

Mitochondrial respiration measurements were performed using Oxygraph-O2k, High-Resolution Respirometry (HRR) (Oroboros Instruments, Austria). All assays were performed at 37 °C with a stirring speed of 750 rpm. Amplified signals from the oxygen sensor were recorded at sampling intervals of 2 s using DatLab-6.1 Software (Oroboros). Air calibration of the respirometer at specific media was performed at air saturation before the commencement of each experiment. Substrates, uncouplers, and specific inhibitors of mitochondrial electron transfer system (ETS) complexes were manually added using Hamilton syringes.

For cardiac mitochondrial respiration measurements, fresh mitochondrial isolate from the whole heart tissue was resuspended in mitochondrial respiration buffer (MiRO 5) consisting of 110 mM sucrose, 60 mM K-lactobionate, 20 mM taurine, 10 mM monobasic potassium phosphate, 3 mM magnesium chloride, 20 mM HEPES, 1 mM EGTA and 0.1% (w/v) BSA at pH 7.1. Since both carbohydrate and fatty acids can compete as a source of substrate for mitochondrial oxidative energy production [23], two different Substrate-Uncoupler-Inhibitor Titration (SUIT) protocols namely fatty acid + carbohydrate substrates and carbohydrate substrates alone were employed [24].

In the fatty acid + carbohydrate protocol (Fig. 1A), the substrates Palmitoyl Carnitine (25 µM), Malate (2 mM), Pyruvate (5 mM), Glutamate (5 mM), and Succinate (10 mM) were added successively at a saturating concentration of 5 mM ADP (state 3 respiration), while in the carbohydrate alone protocol (Fig. 1B), Palmitoyl Carnitine was excluded. Complex-II dependent respiration was measured by inhibiting complex-I respiration using 0.1 µM Rotenone. Finally, Antimycin-A (2.5 µM) was added to inhibit Complex-III-mediated respiration, giving residual oxygen consumption (ROX). For all HRR measurements, Oxygen Consumption Rate (OCR) was expressed in pmol. $s^{-1}$ $mg^{-1}$ of the protein and all the values represented were ROX-corrected.

### Cell culture, cytotoxicity, and cell death analysis with CQ treatment

H9c2, rat embryonic cardiomyoblast cells were maintained in High-Glucose DMEM supplemented with 10% FBS in an atmosphere of 37 °C and 5% $CO_2$. Cytotoxicity of CQ was assessed using Lactate Dehydrogenase (LDH) assay kit (CytoScan, G-Biosciences, USA) and cell death was visualized by fluorescence microscopy (Carl Zeiss AxioObserver 7, Germany) after staining with Hoechst/PI.

### Quantitative real-time PCR

For mitochondrial copy number analysis, total DNA from cells was extracted using the Smart Extract DNA Kit (Eurogentec, Belgium) and the mitochondrial DNA content was assessed by quantitative real-time PCR [25]. For gene expression analysis of the transcription factors related to mitochondrial biogenesis, the total RNA from CQ treated cells for 12 h was isolated using TriXtract (G-Biosciences, USA) and used for cDNA synthesis (iScript cDNA Synthesis Kit, Bio-Rad, USA). qPCR analysis of TFAM, NRF1, NRF2A, NRF2B, TFB1, and TFB2 was done using SYBR GREEN chemistry (TB Green Premix Ex Taq II, Takara) and normalized to β-actin [26]. The assay protocol was optimized and performed in CFX96 Touch Real-Time PCR
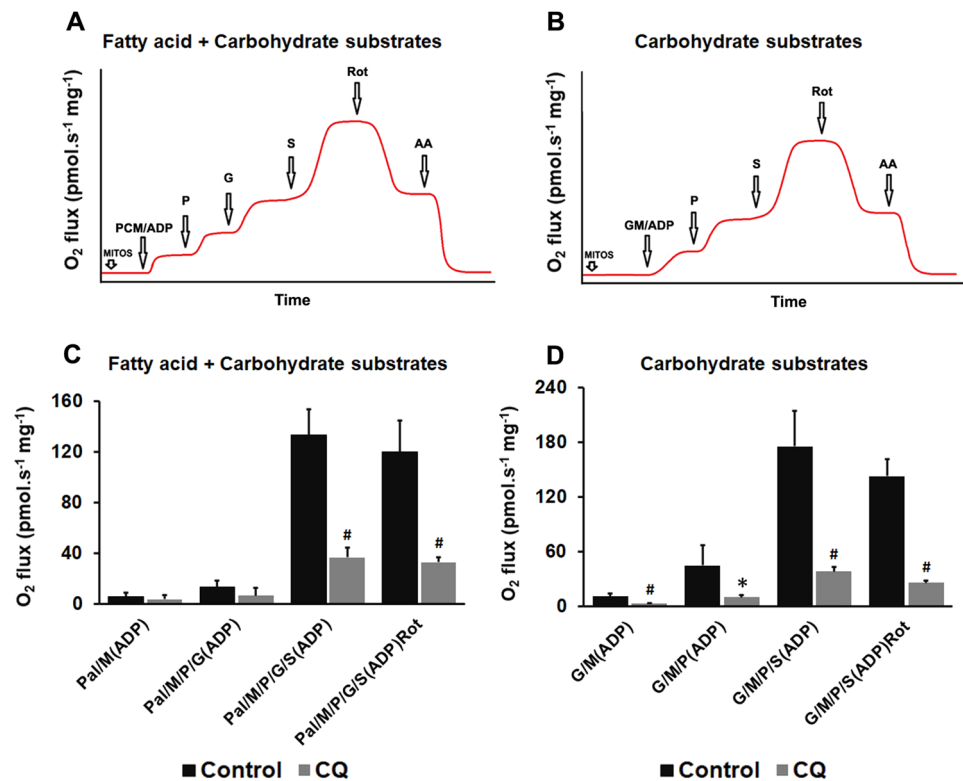
**Fig. 1** Substrate-mediated mitochondrial respiration in isolated cardiac mitochondria, post Chloroquine treatment: High-resolution respirometry was utilized to analyze respiration in isolated mitochondria from whole heart of mice using two SUIT protocols, Fatty acid + carbohydrate protocol (**A**) and Carbohydrate alone protocol (**B**). In the fatty acid + carbohydrate protocol, the substrates were added as follows: Palmitoyl Carnitine (25 μM), Malate (2 mM), Pyruvate (5 mM), Glutamate (5 mM), and Succinate (10 mM) in a sequential manner at saturating concentration of ADP (5 mM), while in the carbohydrate alone protocol, Palmitoyl Carnitine was excluded. With both the protocols state 3 respiration was assessed. **C** State 3 respiration following Fatty acid substrates (Palmitoyl car-

nitine + Malate), Fatty acid + Carbohydrate substrates (Palmitoyl carnitine + Malate + Pyruvate + Glutamate), Fatty acid + carbohydrate substrates for Complex-I and -II (Palmitoyl carnitine + Malate + Pyruvate + Glutamate + Succinate) and state 3 with the sequential addition of Rotenone, Complex-II—linked respiration alone. **D** State 3 respiration following Carbohydrate substrates for Complex-I (Glutamate + Malate & Glutamate + Malate + Pyruvate), Carbohydrate substrates for Complex-I and -II (Glutamate + Malate + Pyruvate + Succinate), and state3 with the sequential addition of Rotenone, Complex-II—linked respiration alone. The bar graphs represent values ± SD. ($n=4$) ($p$ value $\leq 0.05$ as * and $p$ value $\leq 0.001$ as #)

System. Livak method was applied to calculate the normalized expression level of the target gene [27].

## Measurement of mitochondrial membrane potential and mitochondrial superoxide production

Mitochondrial Membrane Potential (MMP) was assessed using TMRE Mitochondrial Membrane Potential Assay (G-Biosciences, USA), and ROS generation from mitochondria was determined using MitoSox Red (Invitrogen, USA). For both assays, CQ-treated cells along with their respective controls were stained as per the manufacturer's protocols and directly subjected to flow-cytometry analysis using BD FAC-SJazz™ (BD Biosciences, USA) with fluorescence intensity recorded with PE emission channel. Cell debris was gated out by distinct forward and side scatter.

## Analysis of mitochondrial morphology

Mitochondrial morphology was assessed with MitoTracker Deep Red FM (Invitrogen, USA). The distribution of fluorescence was imaged at 590 nm excitation/650 nm emission wavelengths using a fluorescence microscope (Carl Zeiss Axio Observer 7, Germany). Images were binarized and the threshold was adjusted for resolving individual mitochondria. Semiquantitative measurements of mitochondrial morphology were done using ImageJ Macro designed by Dagda et al. [28].

## Immunoblot analysis

Whole-cell lysate was prepared in ice-cold RIPA buffer with protease inhibitors (Pierce Biotechnology, USA), followed by protein quantification using BCA-assay kit

(Pierce Biotechnology, USA). The lysates were resolved in SDS-PAGE and transferred onto a PVDF membrane and blocked in 5% skimmed milk in Tris-buffered saline with 0.1% Tween-20. Appropriate dilutions of primary (1:1000 for LC3B, 1:2000 for Vinculin in 3% BSA-TBST) and HRP conjugated secondary antibodies (1:5000 anti-Rabbit IgG) were used, following which the signal was detected using ClarityMax ECL Kit and documented in Gel Doc™ XR Imaging System (Bio-Rad, USA). ImageJ version 1.49a was used for quantification.

## Cellular bioenergetic analysis

H9c2 cells cultured with or without CQ treatment for 24 h were harvested using 0.1% Trypsin–EDTA, washed & resuspended in respiration media, and added to the 2 ml glass chambers (1.5–2 million cells/ml) of O2k-Respirometer.

Intact cell respiration was measured using serum-free cell-culture media. In accordance with Oroboros guidelines [29], coupling control protocol for intact cells was used and the respiration in different coupling control states—ROUTINE (R), LEAK (L), and Maximal respiratory capacity of electron transfer system (E) was derived from the $O_2$ flux values. 'R' corresponding to the physiological respiration of intact cells with endogenous substrates was analyzed after adding cells to the chambers and stabilization of the $O_2$ flux. Oligomycin (2.5 μM), a complex-V inhibitor, was used to measure leak-state (L), the residual respiration independent of ATP synthesis and corresponds to the proton leak, proton slip and cation cycling across the inner mitochondrial membrane. Further, the Oligomycin sensitive respiration, i.e., the difference between 'R' and 'L' (R–L), represents the ATP-linked respiration. Hereafter, the maximal respiration 'E' was attained by stepwise titration of CCCP (Carbonyl cyanide 3-chlorophenylhydrazone), 0.5 μM each time. Spare-capacity of mitochondria was calculated as the difference between the Maximal-capacity and the Routine respiration (E–R). Finally Rotenone (0.1 μM), an inhibitor of Complex-I, and Antimycin A (2.5 μM), an inhibitor of Complex-III were added to the system to inhibit mitochondrial oxygen consumption giving ROX.

Analysis of mitochondrial function following exogenously administered substrates in permeabilized cells was carried out in mitochondrial respiration buffer (MiRO5). For the assessment of respiration linked to individual mitochondrial complexes (state 3 respiration), specific substrates and the inhibitors that feed and/or inhibit each complex were used sequentially. For Complex-I linked respiration, Pyruvate (5 mM), Glutamate (5 mM), and Malate (2 mM) were added followed by Rotenone (0.1 μM). This was followed by the addition of complex-II substrate (10 mM Succinate) and then its inhibitor (Malonate 5 mM) to assay for Complex-II linked respiration; then Antimycin (2.5 μM) was added to

inhibit Complex-III, followed by $N,N,N,N$-Tetramethyl-p-phenylenediamine dihydrochloride (TMPD) (0.5 mM) in the presence of Ascorbate (2 mM), a substrate for Complex-IV and Sodium azide (100 mM) its inhibitor.

## Statistical analysis

Parametric statistics were applied for all data with Student's unpaired $t$ test used for identifying significant differences unless otherwise specified. All tests were performed with the assumptions of two-tailed and homoscedastic sample distribution with data being represented as mean ± standard deviation (SD) from a minimum of three independent experiments. A $p$ value of $< 0.05$ was considered significant.

# Results

## CQ impairs cardiac mitochondrial respiration

Cardiotoxic effects of CQ have been studied in various disease models. However, its impact on mitochondria in normal cardiac tissue remains to be documented completely. We have demonstrated the effects of CQ on isolated cardiac mitochondria using high-resolution respirometry by sequential addition of various respiratory substrates of ETS complexes in two different protocols. In the fatty acid plus carbohydrate protocol, palmitoyl carnitine, malate, glutamate, and pyruvate-dependent state 3 respiration was found to be similar between CQ-treated and control groups (Fig. 1C). But with carbohydrates alone protocol, the state 3 respiration induced by successive addition of glutamate, malate, and pyruvate was significantly lower in CQ treated group (Fig. 1D). Interestingly, in both the protocols, addition of succinate enhanced mitochondrial respiration within as well as between the groups. This implies the significance of mitochondrial complex II in fueling heart tissue as well as the possibility of CQ's detrimental effect on cardiac mitochondria by largely affecting complex II of ETS. This succinate-specific effect was also substantiated by inhibiting the complex I-linked respiration with rotenone.

## CQ alters mitochondrial metabolism in vitro

CQ impaired cardiac mitochondrial respiration in vivo. Thus, to explore the mechanistic basis of how CQ impacts mitochondria under normal conditions, H9c2 cardiomyoblasts were used.CQ treatment for 24 h at 50 μM was chosen for subsequent studies based on preliminary experiments done studying cell viability and autophagosome accumulation as determined by LDH release assay and LC3-II levels, respectively (Fig. 2A–C).
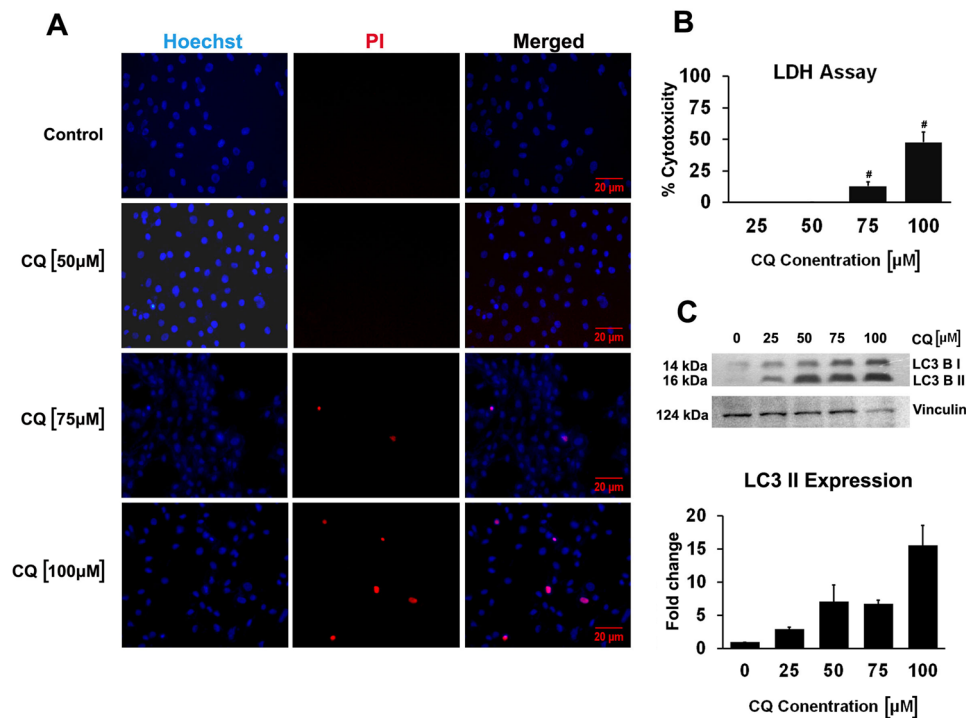
**Fig. 2** Cytotoxicity and LC3—II accumulation with CQ treatment in H9C2 cardiomyoblasts: The cells were exposed for 24 h to High Glucose Media with and without CQ (50 μM) treatments. Cell death and cytotoxicity were analysed by Hoechst/Propidium iodide (H/PI) staining and LDH assay, and LC3 II accumulation assessed through immunoblots was used as a readout for autophagy inhibition. **A** Representative fluorescence images of H/PI staining of H9c2 cells ($n = 3$). Hoechst/Propidium Iodide imaging shows no cell death at 50 μM concentration while with increasing concentrations the cellular toxicity increases. **B** The bar graph shows the % cytotoxicity of CQ at different concentrations. 75 μM and 100 μM CQ caused significant cytotoxicity compared to control, values shown as means $\pm$ SD ($n = 3$). **C** Representative immunoblot for the assessment of LC3 II accumulation. The bar graph shows that 50 μM CQ caused significant autophagic cessation, values shown as means $\pm$ SD ($n = 3$). ($p$ value $\leq 0.05$ as * and $p$ value $\leq 0.001$ as **#**)

The cellular bioenergetic capacity was significantly reduced by CQ as evidenced by decreased mitochondrial respiratory parameters i.e. Routine, Maximal, ATP-linked, and Spare capacity (Fig. 3A, B). This could be due to either a reduction in the availability of metabolic intermediates and/or a decline in the mitochondrial complex function. The Leak to Routine (L/R) and Leak to ETS capacity (L/E) ratio of CQ group compared to control suggests that CQ increased mitochondrial leakiness. Simultaneously, CQ reduced mitochondrial coupling efficiency as indicated by decreased (R-L)/R ratio. In addition, an increase in the fraction of net Routine to ETS capacity i.e., (R-L)/E ratio also indicates a reduction in ETS capacity by CQ (Fig. 3C). The latter calculation was further validated by the observed decrease in complex-I, -III, and –IV dependent respiration induced by their respective substrates on digitonin-permeabilized cells (Fig. 3D).

### CQ increases mitochondrial DNA copy number

The significant decline in mitochondrial respiratory function observed with 24 h exposure to CQ could be due to either a decline in mitochondrial quality or quantity. To resolve this, we analyzed mitochondrial DNA content and genes involved in mitochondrial biogenesis by qPCR. The levels of mitochondrial DNA and the expression of transcription factors associated with mitochondrial biogenesis such as TFAM, TFB1, TFB2, NRF1, NRF2A, and NRF2B were found to be increased in CQ-treated cells (Fig. 4A, B) irrespective of reduced mitochondrial respiratory capacity.

### CQ reduces mitochondrial membrane potential and increase mitochondrial ROS levels

Mitochondrial coupling efficiency is directly associated with its membrane potential as it is the driving force for ATP production by ATP-synthase. To understand the basis of mitochondrial respiratory dysfunction by CQ, MMP was measured by staining cells with TMRM, a cationic dye that accumulates in the mitochondria based on their membrane potential. MMP was found to be reduced in CQ-treated cells irrespective of elevated expression of the genes involved in mitochondrial biogenesis as well as increased mtDNA copy number (Fig. 4C, D). Conversely, MitoSox staining revealed
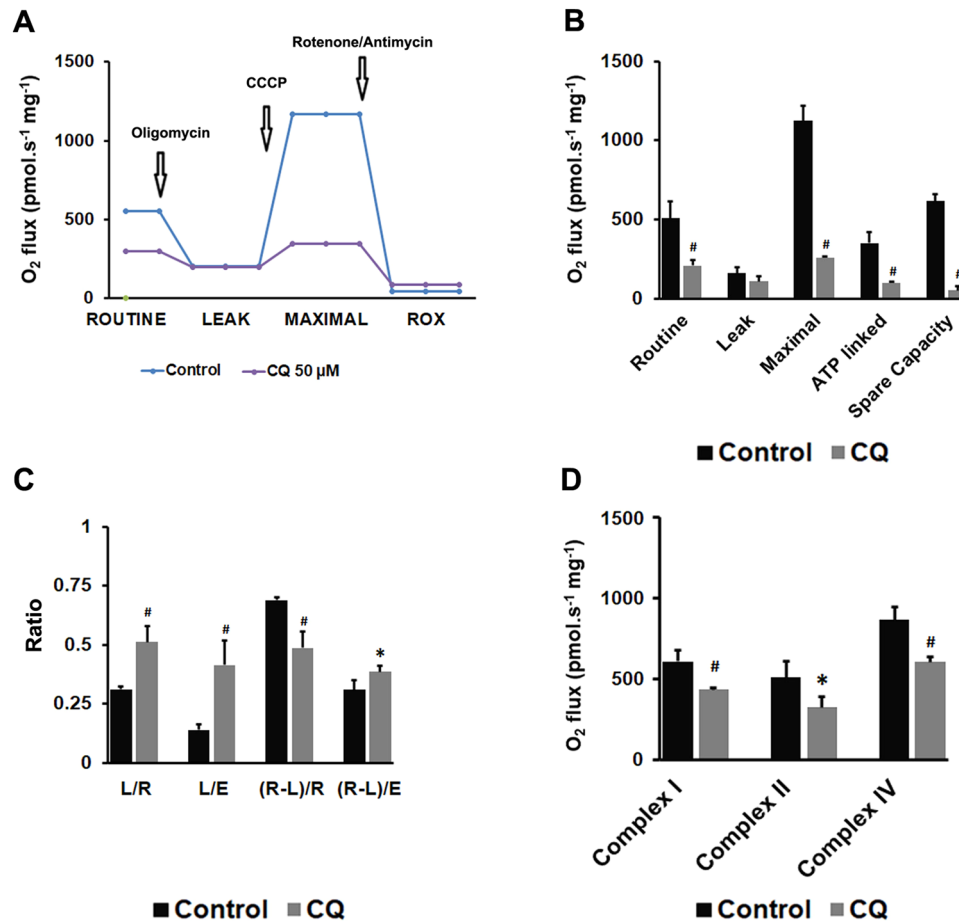
**Fig. 3** CQ treatment results in the deterioration of cellular bioenergetics: The H9c2 cells were given treatments of CQ (50 µM) for 24 h along with respective controls, and the intact cell respiration was measured following resuspension of cells in serum free DMEM in Oroboros Oxygraph. **A** illustration of the experiment as well as the respiratory states measured. **B** Shows the changes in Routine respiration (R), Maximal respiration (E) following uncoupling with CCCP, ATP linked respiration/ATP turnover (R-L) & Reserve capacity/Spare respiratory capacity (E-R). **C** Shows Coupling control ratios (L/R), (L/E), (R-L)/R & (R-L)/E. **D** Activity of the individual complexes of respiratory chain in the presence of exogenous substrates. Complex-I linked respiration with Pyruvate, Glutamate and Malate followed by Rotenone, Complex-II linked respiration following the addition of Succinate and then inhibitor, Malonate, and Complex-IV linked respiration with Ascorbate (2 mM) followed by TMPD, and Sodium azide. The Bar graphs represent values $\pm$ SD ($n=4$). ($p$ value $\leq 0.05$ as * and $p$ value $\leq 0.001$ as #)

an elevated mitochondrial superoxide level in the presence of CQ (Fig. 5A).

### Fragmentation of mitochondria by CQ treatment

With our results pointing towards a defective mitochondrial function with CQ treatment, we went on to assess mitochondrial structure using MitoTracker Deep Red FM-stained cells with a custom-designed macro for NIH ImageJ [28]. This helped in tracing the individual mitochondrial units in an unbiased way and estimating the indices of mitochondrial interconnectivity and mitochondrial elongation. CQ treatment decreased mitochondrial interconnectivity and elongation scores compared to control cells (Fig. 5B, C)

corroborated by significant change in the levels of mitochondrial fusion protein, OPA-1 (Supplementary Fig. 1).

### Discussion

CQ aids in accumulating dysfunctional mitochondria in various disease states possibly due to its effects on autophagy inhibition [19, 30]. Our present study reiterates the same but under normal conditions and at lower daily dosages. Notably, CQ largely impairs succinate-mediated respiration in isolated cardiac mitochondria more than other substrates' mediated respiration (Fig. 1). It has been reported that succinate accumulates in the ischemic heart and enhances ROS generation by undergoing reverse electron transfer during
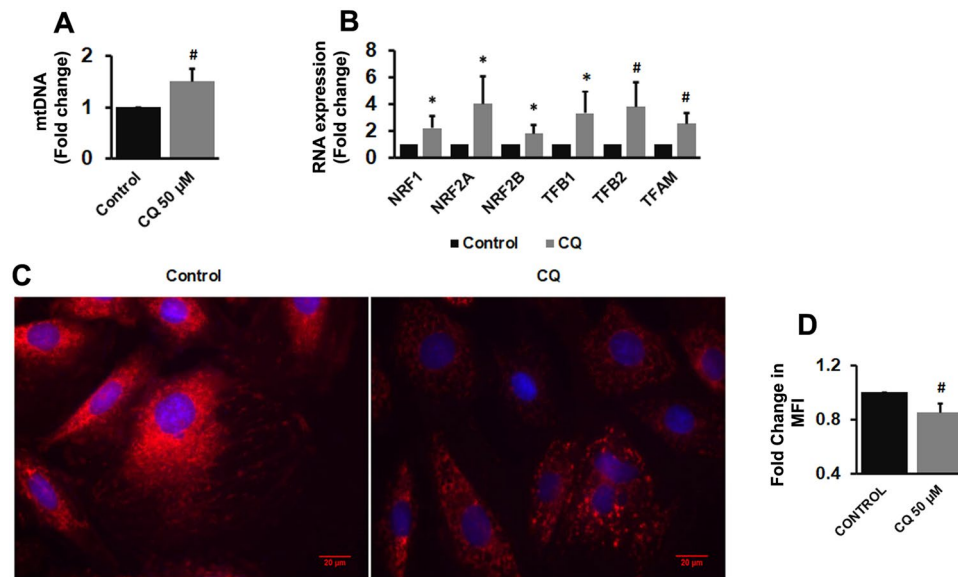
**Fig. 4** Analysis of Mitochondrial DNA content, expression of transcription factors related to mitochondrial biogenesis and mitochondrial membrane potential following CQ treatment: Following CQ (50 μM) treatment, relative mitochondrial content as well as the mRNA expression of transcription factors related to mitochondrial biogenesis was measured by qPCR assay. **A** Mitochondrial content was determined through the quantification of mitochondrial DNA copy number and the bar graph represents the Mitochondrial DNA content normalized to nuclear DNA content as mean $\pm$ SD ($n=5$). **B** Bar graphs represent mRNA expression of transcription factors related to mitochondrial biogenesis estimated by qPCR as mean $\pm$ SD ($n=5$). **C** Representative fluorescence micrographs of H9c2 cells stained with TMRE showing decline in the fluorescence intensity following CQ treatment. **D** The bar graphs represent the fold change in mean values of fluorescence intensity, relative to control, obtained through flow cytometric analysis from three independent experiments ($n=3$) as means $\pm$ SD. ($p$ value $\leq 0.05$ as * and $p$ value $\leq 0.001$ as **#**)

reperfusion [31]. However, succinate-mediated oxygen consumption was not significantly altered in the presence or absence of complex I as well as reverse electron transfer inhibitor, rotenone (Fig. 1). This suggests that CQ largely compromised forward electron transfer in isolated mitochondria under normal conditions. Alternatively, defective succinate utilization induces mitochondrial fragmentation through its release and activation of MFF and Drp1 by inducing GPR91 signaling at the plasma membrane [32]. To demonstrate these possibilities, we have incubated H9c2 cardiomyoblasts with CQ for 24 h and it is observed that CQ compromises routine, maximal, ATP-linked, and spare mitochondrial respiratory capacity (Fig. 3B, C) as well as complex specific mitochondrial respiration (Fig. 3D). This overall decline in the respiratory capacity of mitochondria is associated with reduced MMP (Fig. 4C, D), increased mitochondrial fragmentation, and ROS levels (Fig. 5A–C) irrespective of the counteractive induction of mitochondrial biogenesis as evidenced by elevated mRNA levels of transcription factors related to mitochondrial biogenesis, and an increase in the mitochondrial DNA copy number (Fig. 4A, B).

Autophagy recycles fragmented and dysfunctional mitochondria by engulfing and forming autophagosomes [33]. CQ increases lysosomal pH and thus inhibits autophagic flux by inhibiting the fusion between autophagosomes and lysosomes. This was corroborated by increased accumulation of autophagosomes and decreased autophagic flux as indicated by increased levels of LC3-II and p62, respectively [34]. Likewise, we have also noted increased levels of LC3-II in CQ-treated cells (Fig. 2C) with an accumulation of fragmented mitochondria (Fig. 5) possibly due to defective autophagic flux. Besides autophagic clearance of dysfunctional and fragmented mitochondria, the increase in mitochondrial fusion also ameliorates the mito-toxic effects by supplementing and compensating the defects among fragmented mitochondrial populations. This depends on the proteins regulating mitochondrial fusion dynamics such as OPA -1 which was found to be significantly decreased with CQ treatment (Supplementary Fig. 1). Additionally, it has been reported that increased levels of cholesterol alters biophysical characteristics of mitochondrial membrane by decreasing its fluidity [35]. Since CQ-mediated lysosomal modulation has recently been reported to alter cholesterol distribution in the membrane of the cellular organelle [34], the observed accumulation of fragmented mitochondria could be a result of decreased membrane fluidity and its associated effects on mitochondrial fusion. Recently, Mauthe et al. also demonstrated that CQ and its derivatives affect the intracellular vesicular transport as well as induce severe disorganization
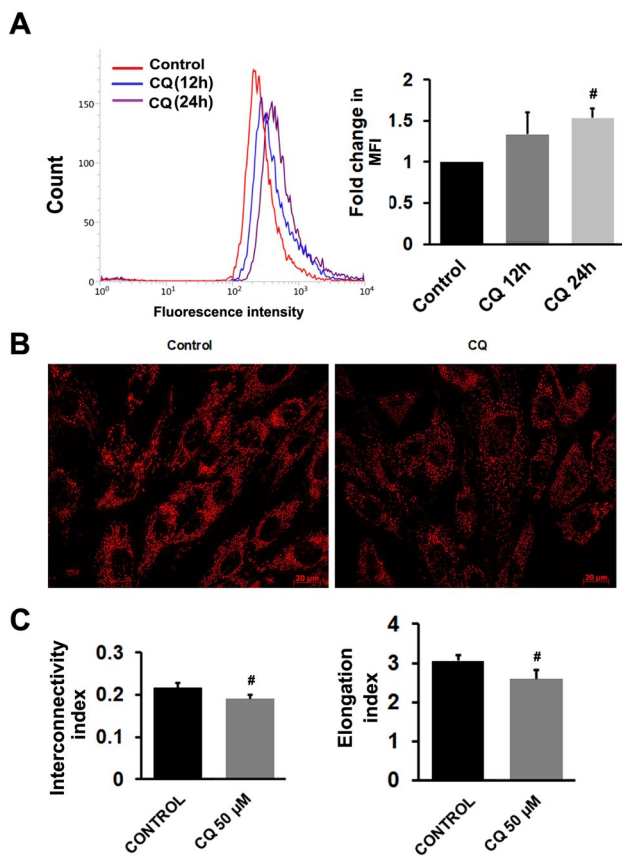
**Fig. 5** CQ treatment results in elevated mitochondrial ROS and mitochondrial fragmentation: **A** Flow cytometry analysis using MitoSox Red shows an increased Mitochondrial superoxide production following CQ treatment. The graphical representation of the flow cytometric data of MitoSox fluorescence are from three independent experiments ($n=3$) as means $\pm$ SD. H9c2 cells given treatments of CQ (50 μM) for 24 h in 8-well chambered coverslips were stained with MitoTracker Red and the Mitochondrial network inter-connectivity and mitochondrial fragmentation was assessed semi-quantitatively. **B** Epifluorescence micrographs of H9c2 cells stained with MitoTracker Red. **C** The bar graphs represent the Mitochondrial network inter-connectivity and mitochondrial elongation indices as mean $\pm$ SD ($n=5$). ($p$ value $\leq 0.05$ as * and $p$ value $\leq 0.001$ as #)

of the Golgi and endo-lysosomal systems at the cellular level in-vitro and in-vivo; probably a similar mechanism by which CQ is causing fragmentation and affecting the mitochondrial network [30]. Also, in concordance with our results that show abnormal mitochondrial fission and deterioration in function, CQ and its derivatives have been shown to induce pathologic responses at the cellular level together with ultra-structural changes like the formation of myeloid and curvilinear inclusion bodies that are shared between cardiopathy and neuropathy [18, 36, 37].

The attempts to include CQ and its derivatives as a treatment modality or as an adjuvant has been fraught with controversies and complications, mostly because of

CQ's reported cardiotoxicity [10]. Recently, observations of cardiac arrhythmias and prolongation of the QT interval associated with CQ treatments have led to caution against the indiscriminate use of these drugs [10, 38, 39]. Generally, cardiotoxicity associated with CQ is studied with high doses of CQ in animal models, which correlates well with the cardiotoxic effect of CQ seen in patients given high doses. But Kanamori et al., 2015 have shown that CQ exerts cardiotoxicity in diabetic models (Type 1 & Type 2) even at a lower dosage (10 mg/kg/day) that is clinically relevant and echoes the question of cardiovascular safety in humans [11]. Even though our study is limited to the mito-toxic effects of CQ in cardiac cells, we believe that it would add to the knowledge and is clinically significant, as CQ is a potential choice for drug repurposing against various viral pathogens and as combinatorial therapies alongside anticancer agents.

In summary, CQ affects substrate-mediated mitochondrial respiration in cardiac cells and causes the deterioration of a healthy mitochondrial population. This could aggravate the pre-existing disproportion in metabolic demand and cardiac output, as observed in conditions like cancer chemotherapeutics-induced heart ailments, rheumatic heart disease, COVID-19, etc., with accompanying cardiopulmonary derangement. This warrants the need for more in-depth and detailed studies in in-vivo systems to unravel the cardiotoxicity of CQ and its derivatives. We further acknowledge the limitations of this study—the effects of CQ on the functional aspect of cardiac tissue need to be studied and correlated, along with the exploration of other plausible pathways involved in the impairment of mitochondrial quality control with CQ treatment. Nevertheless, our study suggests that CQ causes mitochondrial toxicity in healthy cardiac cells and this would be an added burden in conditions with metabolic abnormalities, thus cautioning against the indiscriminate use of this drug.

**Author contributions** The authors confirm their contribution to the paper as follows:Study conception and design: SA and GS; Data collection: SA and SRR; Analysis and interpretation of results: SA, and SM; Draft manuscript preparation: SA, SM, and GS.All authors reviewed the results and approved the final version of the manuscript.

## Declarations

**Conflict of interest** The authors have no conflict of interest.

## References

1. Liu T, Zhang J, Li K et al (2020) Combination of an autophagy inducer and an autophagy inhibitor: a smarter strategy emerging in cancer therapy. Front Pharmacol 11:408. https://doi.org/10.3389/fphar.2020.00408
2. McChesney EW (1983) Animal toxicity and pharmacokinetics of hydroxychloroquine sulfate. Am J Med 75:11–18. https://doi.org/10.1016/0002-9343(83)91265-2
3. Wolpin BM, Rubinson DA, Wang X et al (2014) Phase II and pharmacodynamic study of autophagy inhibition using hydroxychloroquine in patients with metastatic pancreatic adenocarcinoma. Oncologist 19:637–638. https://doi.org/10.1634/theoncologist.2014-0086
4. Schlesinger PH, Krogstad DJ, Herwaldt BL (1988) Antimalarial agents: mechanisms of action. Antimicrob Agents Chemother 32:793–798
5. Li Y, Cao F, Li M et al (2018) Hydroxychloroquine induced lung cancer suppression by enhancing chemo-sensitization and promoting the transition of M2-TAMs to M1-like macrophages. J Exp Clin Cancer Res 37:259. https://doi.org/10.1186/s13046-018-0938-5
6. Wang W, Liu L, Zhou Y et al (2019) Hydroxychloroquine enhances the antitumor effects of BC001 in gastric cancer. Int J Oncol 55:405–414. https://doi.org/10.3892/ijo.2019.4824
7. Li C, Zhu X, Ji X et al (2017) Chloroquine, a FDA-approved drug, prevents Zika virus infection and its associated congenital microcephaly in mice. EBioMedicine 24:189–194. https://doi.org/10.1016/j.ebiom.2017.09.034
8. Chatre C, Roubille F, Vernhet H et al (2018) Cardiac complications attributed to chloroquine and hydroxychloroquine: a systematic review of the literature. Drug Saf 41:919–931. https://doi.org/10.1007/s40264-018-0689-4
9. Blignaut M, Espach Y, van Vuuren M et al (2019) Revisiting the cardiotoxic effect of chloroquine. Cardiovasc Drugs Ther 33:1–11. https://doi.org/10.1007/s10557-018-06847-9
10. Mubagwa K (2020) Cardiac effects and toxicity of chloroquine: a short update. Int J Antimicrobial Agents 56:106057. https://doi.org/10.1016/j.ijantimicag.2020.106057
11. Kanamori H, Takemura G, Goto K et al (2015) Autophagic adaptations in diabetic cardiomyopathy differ between type 1 and type 2 diabetes. Autophagy 11:1146–1160. https://doi.org/10.1080/15548627.2015.1051295
12. Dutta D, Calvani R, Bernabei R et al (2012) Contribution of impaired mitochondrial autophagy to cardiac aging: mechanisms and therapeutic opportunities. Circ Res 110:1125–1138. https://doi.org/10.1161/CIRCRESAHA.111.246108
13. Levine B, Klionsky DJ (2004) Development by self-digestion: molecular mechanisms and biological functions of autophagy. Dev Cell 6:463–477. https://doi.org/10.1016/S1534-5807(04)00099-1
14. Rifki OF, Hill JA (2012) Cardiac autophagy: good with the bad. J Cardiovasc Pharmacol 60:248–252. https://doi.org/10.1097/FJC.0b013e3182646cb1
15. Lampert MA, Gustafsson ÅB (2018) Balancing autophagy for a healthy heart. Curr Opin Physiol 1:21–26. https://doi.org/10.1016/j.cophys.2017.11.001
16. Chaanine AH, Gordon RE, Nonnenmacher M et al (2015) High-dose chloroquine is metabolically cardiotoxic by inducing lysosomes and mitochondria dysfunction in a rat model of pressure overload hypertrophy. Physiol Rep 3:e12413. https://doi.org/10.14814/phy2.12413
17. Di Girolamo F, Claver E, Olivé M et al (2018) Dilated cardiomyopathy and hydroxychloroquine-induced phospholipidosis: from curvilinear bodies to clinical suspicion. Rev Esp Cardiol 71:491–493. https://doi.org/10.1016/j.rec.2017.04.017
18. Khosa S, Khanlou N, Khosa GS, Mishra SK (2018) Hydroxychloroquine-induced autophagic vacuolar myopathy with mitochondrial abnormalities. Neuropathology 38:646–652. https://doi.org/10.1111/neup.12520
19. Redmann M, Benavides GA, Berryhill TF et al (2017) Inhibition of autophagy with bafilomycin and chloroquine decreases mitochondrial quality and bioenergetic function in primary neurons. Redox Biol 11:73–81. https://doi.org/10.1016/j.redox.2016.11.004
20. Soong TR, Barouch LA, Champion HC et al (2007) New clinical and ultrastructural findings in hydroxychloroquine-induced cardiomyopathy–a report of 2 cases. Hum Pathol 38:1858–1863. https://doi.org/10.1016/j.humpath.2007.06.013
21. Essien EE, Ette EI (1986) Effects of chloroquine and didesethylchloroquine on rabbit myocardium and mitochondria. J Pharm Pharmacol 38:543–546. https://doi.org/10.1111/j.2042-7158.1986.tb04635.x
22. MiPNet20.06 IsolationMouseHeart-mt - Bioblast. https://wiki.oroboros.at/index.php/MiPNet20.06_IsolationMouseHeart-mt. Accessed 14 Feb 2021
23. Lopaschuk GD, Ussher JR (2016) Evolving concepts of myocardial energy metabolism. Circ Res 119:1173–1176. https://doi.org/10.1161/CIRCRESAHA.116.310078
24. Jayakumari NR, Rajendran RS, Sivasailam A et al (2021) Honokiol regulates mitochondrial substrate utilization and cellular fatty acid metabolism in diabetic mice heart. Eur J Pharmacol 896:173918. https://doi.org/10.1016/j.ejphar.2021.173918
25. Wu B, Ni H, Li J et al (2017) The impact of circulating mitochondrial DNA on cardiomyocyte apoptosis and myocardial injury after TLR4 activation in experimental autoimmune myocarditis. Cell Physiol Biochem 42:713–728. https://doi.org/10.1159/000477889
26. Lin S, Wu X, Tao L et al (2015) The metabolic effects of traditional Chinese medication Qiliqiangxin on H9C2 cardiomyocytes. Cell Physiol Biochem 37:2246–2256. https://doi.org/10.1159/000438580
27. Livak KJ, Schmittgen TD (2001) Analysis of relative gene expression data using real-time quantitative PCR and the $2^{-\Delta\Delta CT}$ method. Methods 25:402–408. https://doi.org/10.1006/meth.2001.1262
28. Dagda RK, Cherra SJ, Kulich SM et al (2009) Loss of PINK1 function promotes mitophagy through effects on oxidative stress and mitochondrial fission. J Biol Chem 284:13843–13855. https://doi.org/10.1074/jbc.M808515200
29. MiPNet08.09 CellRespiration—Bioblast. https://wiki.oroboros.at/index.php/MiPNet08.09_CellRespiration. Accessed 19 Feb 2021
30. Mauthe M, Orhon I, Rocchi C et al (2018) Chloroquine inhibits autophagic flux by decreasing autophagosome-lysosome fusion. Autophagy 14:1435–1455. https://doi.org/10.1080/15548627.2018.1474314
31. Zhang J, Wang YT, Miller JH et al (2018) Accumulation of succinate in cardiac ischemia primarily occurs via canonical krebs cycle activity. Cell Rep 23:2617–2628. https://doi.org/10.1016/j.celrep.2018.04.104
32. Lu Y-T, Li L-Z, Yang Y-L et al (2018) Succinate induces aberrant mitochondrial fission in cardiomyocytes through GPR91 signaling. Cell Death Dis 9:672. https://doi.org/10.1038/s41419-018-0708-5
33. Zhang J (2013) Autophagy and mitophagy in cellular damage control. Redox Biol 1:19–23. https://doi.org/10.1016/j.redox.2012.11.008

34. Rajasekaran S, Ramaian Santhaseela A, Ragunathan S et al (2022) Altered lysosomal function manipulates cellular biosynthetic capacity by remodeling intracellular cholesterol distribution. Cell Biochem Biophys. https://doi.org/10.1007/s12013-022-01123-y

35. Colell A, García-Ruiz C, Lluis JM et al (2003) Cholesterol impairs the adenine nucleotide translocator-mediated mitochondrial permeability transition through altered membrane fluidity. J Biol Chem 278:33928–33935. https://doi.org/10.1074/jbc.M210943200

36. Siddiqui AK, Huberfeld SI, Weidenheim KM et al (2007) Hydroxychloroquine-induced toxic myopathy causing respiratory failure. Chest 131:588–590. https://doi.org/10.1378/chest.06-1146

37. Stein M, Bell MJ, Ang LC (2000) Hydroxychloroquine neuromyotoxicity. J Rheumatol 27:2927–2931

38. Uzelac I, Iravanian S, Ashikaga H et al (2020) Fatal arrhythmias: another reason why doctors remain cautious about chloroquine/hydroxychloroquine for treating COVID-19. Heart Rhythm 17:1445–1451. https://doi.org/10.1016/j.hrthm.2020.05.030

39. Jankelson L, Karam G, Becker ML et al (2020) QT prolongation, torsades de pointes, and sudden death with short courses of chloroquine or hydroxychloroquine as used in COVID-19: a systematic review. Heart Rhythm 17:1472–1479. https://doi.org/10.1016/j.hrthm.2020.05.008